Journal of Physics: Conference Series **167** (2009) 012068 doi:10.1088/1742-6596/167/1/012068

Monte Carlo study of the double and super-exchange model with lattice distortion

J R Suárez[1], E Vallejo[1], O Navarro[1] and M Avignon[2]

[1]Instituto de Investigaciones en Materiales, Universidad Nacional Autónoma de México, Apartado Postal 70-360, 04510 México D. F., México.
[2]Institut Néel, Centre National de la Recherche Scientifique (CNRS) and Université Joseph Fourier, BP 166, 38042 Grenoble Cedex 9, France.

E-mail: jrsuarez@iim.unam.mx

Abstract. In this work a magneto-elastic phase transition was obtained in a linear chain due to the interplay between magnetism and lattice distortion in a double and super-exchange model. It is considered a linear chain consisting of localized classical spins interacting with itinerant electrons. Due to the double exchange interaction, localized spins tend to align ferromagnetically. This ferromagnetic tendency is expected to be frustrated by anti-ferromagnetic super-exchange interactions between neighbor localized spins. Additionally, lattice parameter is allowed to have small changes, which contributes harmonically to the energy of the system. Phase diagram is obtained as a function of the electron density and the super-exchange interaction using a Monte Carlo minimization. At low super-exchange interaction energy phase transition between electron-full ferromagnetic distorted and electron-empty anti-ferromagnetic undistorted phases occurs. In this case all electrons and lattice distortions were found within the ferromagnetic domain. For high super-exchange interaction energy, phase transition between two site distorted periodic arrangement of independent magnetic polarons ordered anti-ferromagnetically and the electron-empty anti-ferromagnetic undistorted phase was found. For this high interaction energy, Wigner crystallization, lattice distortion and charge distribution inside two-site polarons were obtained.

1. Introduction

Theoretical studies to explain the ferromagnetism of manganites are widely based on the so-called double exchange (DE) model introduced by Zener [1, 2]. The origin of the DE mechanism lies in the intra-atomic Hund's spin coupling J_H between itinerant and localized electrons [1, 2, 3, 4, 5]. The key point is that this coupling implies that the hopping depends on the configuration of the neighbor spins and explains how carriers improve their kinetic energy by forcing the localized spins to become ferromagnetically ordered. This ferromagnetic (F) tendency is expected to be frustrated by anti-ferromagnetic (AF) super-exchange (SE) interactions between localized spins $\overrightarrow{S}_i$ as first discussed by de Gennes [6] who conjectured the existence of canted states. Since then, it has become clear that microstructured spin configurations exist instead of macroscopic canted states resulting from such competition. Recently, an unifying picture in one dimension (1D) for classical local spins has shown the existence of two and three-sites ferromagnetic polarons separated by AF links in the whole range of electron density [7, 8]. As a result of the spin dependent hopping, carriers are localized in the ferromagnetic bonds, giving rise to bond ordered states for commensurate fillings. In turn, this will induce significant lattice distortions in systems

in which the electrons interact with the lattice by affecting the hopping amplitude as in the Su-Schrieffer-Heeger (SSH) model [9, 10]. This point implies an important connection between the magnetic structure and lattice distortions. Recently, Vallejo et al. [11, 12, 13] have shown that three-leg ladders in the oxyborate system Fe_3BO_5 may provide evidence for the interplay between the magnetic structure and the observed structural and charge ordering transition, such that long and short bonds on the rungs alternate along the ladder axis [14]. In this Fe-ludwigite X-ray diffraction studies show contraction of the rungs [15].

The main goal of this work is to study the interplay between magnetic interactions and lattice distortion in one-dimensional systems. We consider the SSH model for the electron-lattice coupling together with the double and super-exchange model. As in [7] we will determine the phase diagram as a function of the band filling, the super-exchange interaction energy and we will also examine the effect of including coupling with the lattice.

We consider the exchange Hamiltonian to describe the localized and itinerant electrons [5, 16],

$$H = -\sum_i t_{i,i+1} \cos\left(\frac{\theta_{i,i+1}}{2}\right)(c_i^+ c_{i+1} + h.c.) + J\sum_i \vec{S}_i \cdot \vec{S}_{i+1}, \tag{1}$$

where $c_i^+(c_i)$ are the fermions creation (annihilation) operators of conduction electrons at site i, $t_{i,i+1}$ is the nearest-neighbor (n.n) hopping parameter and $\vec{S}_i$ is the localized spin at site i. The first term represents the DE contribution favouring F ordering of local spins. The last term is a SE coupling between n.n localized spins $\vec{S}_i$, J being an AF interaction energy which stabilizes an AF phase for $x = 0$ and competes with DE for intermediate fillings. In this approach we consider the local spins as classical, $\vec{S}_i \to \infty$, a reasonable approximation in many cases in view of the similarity with the well known results [17, 18, 19, 20]. Itinerant electrons are either parallel or antiparallel to the local spins are thus *spinless*. Finally, $\theta_{i,i+1}$ $(0 \leq \theta_{i,i+1} \leq \pi)$ is the relative angle between the classical localized spins at sites i and $i+1$.

Now we introduce the effect of bond deformation on the itinerant electrons. In the SSH model, the complicated inter-atomic potential is represented using the electron-lattice coupling constant $g_t \simeq \partial t/\partial y$ $(g_t < 0)$ which describes the change of the hopping amplitude under a small change of the n.n bond length y,

$$H_{e-l} = g_t \sum_i y_{i,i+1}(c_i^+ c_{i+1} + h.c.) + \frac{K_t}{2}\sum_i y_{i,i+1}^2, \tag{2}$$

$y_{i,i+1}$ is the change of the $i, i+1$ lattice distance. It is important to mention that the original equilibrium lattice spacing a_0 (and so is t) in the absence of H_{e-l} results from the bonding produced by all other electrons in the system except the itinerant ones that we are considering in (1). The elastic constant K_t refers to this equilibrium lattice.

The electron-lattice part may be written in the following standard form, introducing the dimensionless parameters for the deformation $\delta_{i,i+1} = g_t y_{i,i+1}/t$ and the usual coupling constant $\lambda = 2g_t^2/\pi t K_t$:

$$H_{e-l} = -t\sum_i \delta_{i,i+1}(c_i^+ c_{i+1} + h.c.) + \frac{t}{\pi\lambda}\sum_i \delta_{i,i+1}^2. \tag{3}$$

The hopping term changes as $t_{i,i+1} = t\,(1 + \delta_{i,i+1})$ with $|\delta_{i,i+1}| \ll 1$. The complete Hamiltonian is given by

$$\begin{aligned} H &= -t\sum_i (1+\delta_{i,i+1}) \cos\left(\frac{\theta_{i,i+1}}{2}\right)(c_i^+ c_{i+1} + h.c.) \\ &\quad + JS^2 \sum_i \cos(\theta_{i,i+1}) + B\sum_i \delta_{i,i+1}^2, \end{aligned} \tag{4}$$

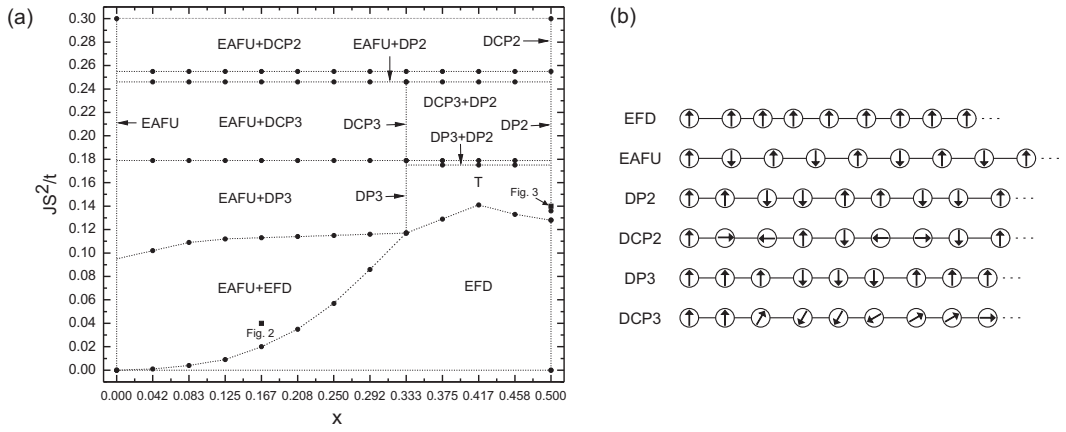

Figure 1. (a) Magneto-elastic phase diagram as a function of the SE interaction energy JS^2/t and the conduction electron density x, for a typical value of the elastic energy $B/t = 30$. A dotted line in this diagram represents a guide for the eyes. (b) Partial spin configuration snapshot of the different phases is also shown. The phases are described in the text.

where $B/t = 1/\pi\lambda$. Due to the dependence of the hopping amplitude on the spin configuration, the contribution of the itinerant electrons to the metallic bonding varies with the magnetic state and so will do the resulting lattice spacing.

2. Numerical results and discussion

The phase diagram for the model given by (4) is obtained as a function of the conduction electron density x ($0 \leq x \leq 0.5$ because of hole-electron symmetry) and the SE interaction energy J. $T = 0K$ and open boundary conditions on a linear chain of $N = 24$ sites were used. $N-1$ angles $\theta_{i,i+1}$ and $N-1$ values of $\delta_{i,i+1}$ had to be optimized. For this goal, we used an analytical optimization and a classical Monte Carlo method. The analytical solution was tested as a starting point in the Monte Carlo simulation. The whole magneto-elastic phase diagram obtained here is shown in figure 1(a). Partial spin configuration snapshot of the most important phases is shown in figure 1(b). For low super-exchange interaction energy, $JS^2/t \lesssim 0.11$, an electron-full ferromagnetic distorted (EFD) and an electron-empty anti-ferromagnetic undistorted (EAFU) phase transition was found. Analytical optimization implies angles $\theta_{i,i+1} = 0$ exactly for the EFD phase. For commensurate electronic fillings at $x = 1/3$ and at $x = 1/2$ displacements look like Peierls distortion. Because of the typical value of the elastic energy, uniform displacements ($\delta_U = \sin(\pi x)/(\pi B/t)$) and uniform charge distribution ($n_i = x$) are expected in the thermodynamic limit ($N \to \infty$). The $\delta_{i,i+1} = 0$ displacement and $\theta_{i,i+1} = \pi$ angle solutions were obtained for EAFU phase at $x = 0$. Phase separation (EAFU+EFD in figures 1(a) and 2) between EFD and EAFU phases, consist of one large electron-full F distorted polaron within an electron-empty AF undistorted background. Charge distributions n_i are also presented. Analytical optimization implies angles 0 and π exactly for the ferromagnetic and anti-ferromagnetic domains respectively. In the limit $B/t \to \infty$, the magnetic-only F-AF phase transition was previously reported [7]. Above EAFU+EFD phase separation, another phase separation (EAFU+DP3) between T-phase (for high conduction electron density) and EAFU phase (for $x = 0$) can be observed in figure 1(a). T-phase is a more general complex distorted phase found by the Monte Carlo method and can be polaronic like or not. At $x = 1/2$

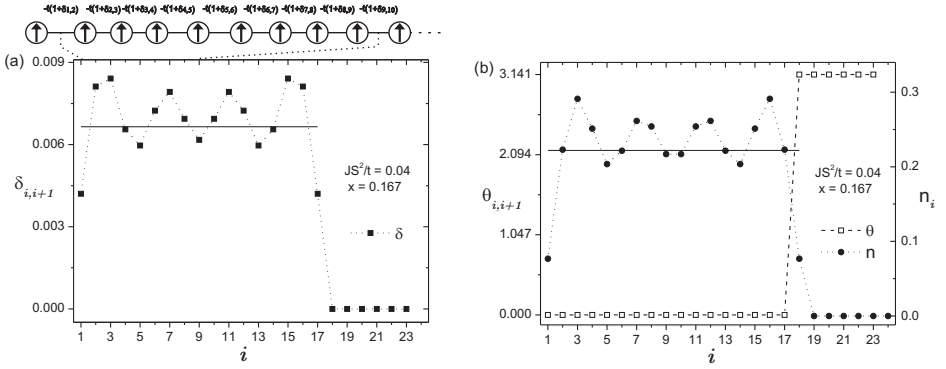

Figure 2. EAFU+EFD phase separation for 4 electrons ($x = 0.167$) and $JS^2/t = 0.04$ showing: (a) $\delta_{i,i+1}$ and (b) angles and charge distribution. Partial spin configuration snapshot is also shown.

and at $x = 1/3$ T-phase becomes basically DP2 (see figure 3) and DP3 phases respectively. DP2 and DP3 phases are two and three-site-distorted periodic arrangement of independent F polarons ordered anti-ferromagnetically. DP2 and DP3 are magneto-elastic Peierls phases. Displacements are $(2B/t)^{-1} \sim 0.0167$ and $(2\sqrt{2}B/t)^{-1} \sim 0.0118$ for DP2 and DP3 phases respectively. EAFU+DP3 phase separation is degenerate with phases where the polarons can be ordered or not, while keeping the number of F and AF bonds fixed; phases obtained within the "spin-induced Peierls instability" [21] belong to this class. The former degeneracy unifies ideas like phase separation and individual polarons and gives a natural response to the instability at the Fermi energy and to an infinite compressibility as well. It is worth to notice that in the magnetic-only case, a phase AF+P3 (similar to EAFU+DP3) was identified using $S = 3/2$ quantum spins [22]. P2 and P3 phases were also previously reported for classical [7, 21] and $S = 1/2$ quantum [17] local spins. Figure 1(a) shows EAFU+DP3 phase separation for a typical value of the SE interaction energy $JS^2/t = 0.14$. There is a single electron inside each three-site independent magnetic polaron, so a Wigner crystallization is formed. For DP3 and EAFU+DP3 phases, we find lattice distortion within each three-site magnetic polaron. For high SE interaction energy, DP3 and DP2 become DCP3 and DCP2 canted phases (distorted canted P3 and P2 phases respectively). In the absence of electron-lattice interaction (limit $B/t \to \infty$), the CP3 phase present a continuos angular degeneracy [7]. Now, this degeneracy is broken by the lattice distortion. Instead of the continuos degeneracy, only four set of angles inside each CP3 polaron were found [23]. For instance, DCP3 phase in figure 1(a) is a distorted canted phase with angles 0 and θ. Displacements decrease when $\theta \to \pi$. The expected DP2-DCP3, DCP3-EAFU and DP2-EAFU phase transitions are also obtained for values of the SE interaction energy above the T-EAFU phase transition (see figure 1(a)). Finally, the DCP2-EAFU phase transition occurs for high SE interaction energy $JS^2/t > 0.2542$. DCP2 phase becomes AFU (anti-ferromagnetic undistorted) in the limit $JS^2/t \to \infty$. In this phase each electron is trapped in a single site forming a Wigner crystallization. It is important to mention that the size chosen for the linear chain (N=24 sites), does not change the nature of the phases involved in the phase diagram.

In conclusion we have studied the rich phase diagram resulting from the interplay between magnetic interactions and lattice distortion within an exchange model in one-dimensional systems using large Hund's coupling and classical localized spins. Basically, microstuctured phases with small ferromagnetic polarons result from the double and super-exchange interaction. Our results for low SE interaction energy show phase separation between ferromagnetic and anti-ferromagnetic phases. In this case, the ferromagnetic domain contains all the electrons

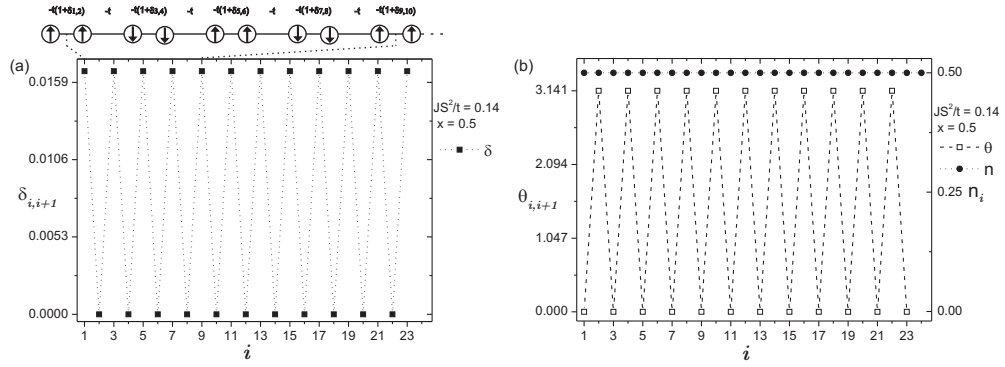

Figure 3. DP2 phase at $x = 0.5$ showing (a) $\delta_{i,i+1}$ and (b) angles and charge distribution. Partial spin configuration snapshot is also shown.

and a lattice contraction occurs only within this domain. For larger SE interaction energy, we found phase separations involving small two and three-site distorted polarons, in which a Wigner crystallization can be identified. The important magneto-elastic effect obtained here leads to local bond contractions that consequently change the lattice parameters which should be observable. We expect this effect to occur in low-dimensional systems in which magnetic ions coupled via a double-exchange type interaction are present, as for example molecular magnets, halogen bridged metal chains or charge transfer salts. Ladders in the ludwigite family seem to be good candidates also.

Acknowledgments

We want to acknowledge partial support from CONACyT Grant-57929 and PAPIIT-IN108907 from UNAM. E. V. acknowledge DGAPA-UNAM for financial support.

References

[1] Zener C 1951 *Phys. Rev.* **82** 403
[2] Zener C 1951 *Phys. Rev.* **81** 440
[3] Jonker G H and Van Santen J H 1950 *Physica* **16** 337
[4] Jonker G H and Van Santen J H 1950 *Physica* **16** 599
[5] Anderson P W and Hasegawa H 1955 *Phys. Rev.* **100** 675
[6] de Gennes P G 1960 *Phys. Rev.* **118** 141
[7] Vallejo E, López-Urías F, Navarro O and Avignon M 2008 *J. Magn. Magn. Mater.* **320** e425
[8] Vallejo E, López-Urías F, Navarro O and Avignon M 2009 *Solid State Commun.* **149** 126
[9] Su W P, Schrieffer J R and Heeger A J 1979 *Phys. Rev. Lett.* **42** 1698
[10] Su W P, Schrieffer J R and Heeger A J 1980 *Phys. Rev.* B **22** 2099
[11] Vallejo E and Avignon M 2006 *Phys. Rev. Lett.* **97** 217203
[12] Vallejo E and Avignon M 2007 *Rev. Mex. Fís.* S **53** (7) 1
[13] Vallejo E and Avignon M 2007 *J. Magn. Magn. Mater.* **310** 1130
[14] Mir M *et al.* 2001 *Phys. Rev. Lett.* **87** 147201
[15] Mir M, Janczak J and Mascarenhas Y P 1996 *J. Appl. Cryst.* **39** 1356
[16] Müller-Hartmann E and Dagotto E 1996 *Phys. Rev.* B **54** R6819
[17] Garcia D J *et al.* 2000 *Phys. Rev. Lett.* **85** 3720
[18] Garcia D J *et al.* 2002 *Phys. Rev.* B **65** 134444
[19] Yunoki S *et al.* 1998 *Phys. Rev. Lett.* **80** 845
[20] Dagotto E *et al.* 1998 *Phys. Rev.* B **58** 6414
[21] Koshibae W, Yamanaka M, Oshikawa M and Maekawa S 1999 *Phys. Rev. Lett.* **82** 2119
[22] Neuber D R *et al.* 2006 *Phys. Rev.* B **73** 014401
[23] Vallejo E 2008 *Microelectron. J.* **39** 1266